ChemComm

COMMUNICATION

View Article Online
View Journal | View Issue

Cite this: *Chem. Commun.*, 2025, **61**, 8687

Received 10th April 2025,
Accepted 6th May 2025

DOI: 10.1039/d5cc02019k

rsc.li/chemcomm

Freed from iron: easy release of a stable ketene from the reaction of CO with di-iron bis-μ²-alkylidenes†

Sandip Munshi, ‡[a] Raphaël Ravel-Massol, ‡[a] Ricardo Garcia-Serres, [b] Nicolas Suaud, [c] Rémi Maurice, [d] Nathalie Saffon-Merceron, [e] Nicolas Mézailles *[a] and Marie Fustier-Boutignon *[a]

Iron bis-μ²-alkylidene complexes were shown to perform CO/alkylidene coupling and liberate a stable ketene derivative. The easy release of the ketene formed from CO incorporation is usually the prerogative of terminal iron carbene complexes, while dimetallic, bridging carbenes tend to retain bridging acyl ligands after 1,1 migratory insertion of CO. Observations at −40 °C showed that an acyl intermediate could evolve into a ketene and form a stable μ²-alkylidene di-iron hexacarbonyl complex. Ketene release was shown to depend on the redox state of the iron byproducts. The C=C bond formation is reversible, with instant hydration–decarboxylation upon water addition at room temperature.

The interaction of carbon monoxide with organometallic complexes of early transition metals, and particularly iron, has been a topic of abundant research over the years, from the understanding of the reaction mechanisms in heterogeneous Fischer–Tropsch synthesis[1,2] to the development of sustainable hydroformylation reaction catalysts.[3,4] These somewhat distant catalytic processes are related to each other by the co-existence of a CO ligand with alkyl- and/or alkylidene-type ligands at the surface or in the coordination sphere of iron. In homogeneous conditions, terminal and bridging alkylidenes are differentiated by their reactivity, especially toward CO. Terminal carbenes/alkylidenes are classically known to lead to the formation of ketenes by direct carbonylation *via* 1,1 insertion at an sp^2 carbon (Scheme 1A, eqn (1)).[5] This reactivity is often used to illustrate the carbenic character of ligands or intermediates[6–9]

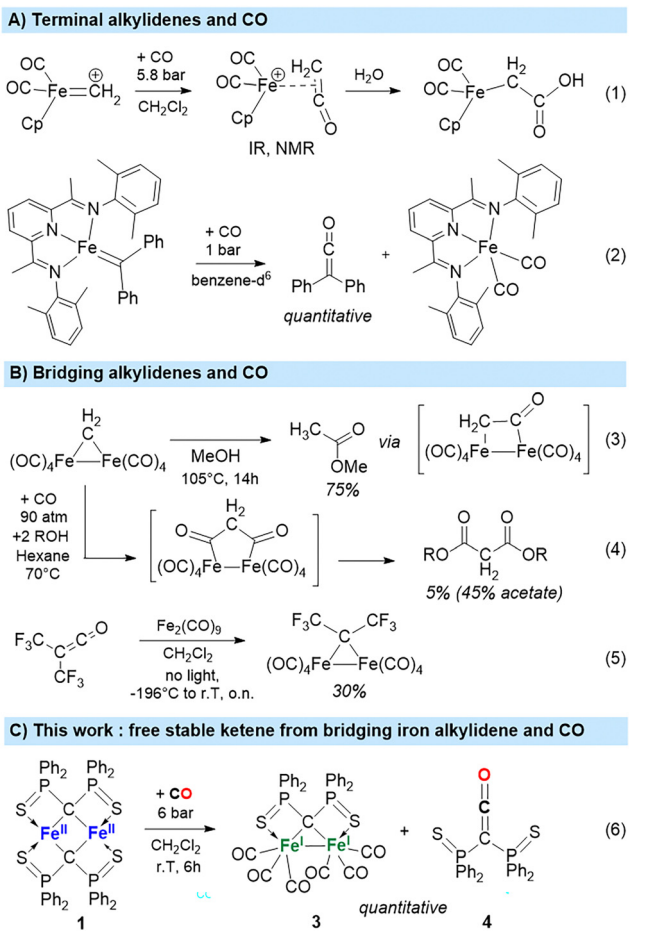

Scheme 1 Usual reactivity of CO to (A) terminal *vs.* (B) bridging iron alkylidene, and (C) bridging iron bis-alkylidene (this work).

[a] *Université de Toulouse, CNRS, LHFA - UMR 5069, 118 Route de Narbonne, 31062 Toulouse, France. E-mail: marie.fustier-boutignon@univ-tlse3.fr*
[b] *Université Grenoble Alpes, CNRS, CEA, IRIG, Laboratoire de Chimie et Biologie des Métaux, 17 rue des Martyrs, 38000 Grenoble, France*
[c] *Université de Toulouse, CNRS, LCPQ, 118 Route de Narbonne, 31062 Toulouse, France*
[d] *Univ Rennes, CNRS, ISCR (Institut des Sciences Chimiques de Rennes) – UMR 6226, F-35000 Rennes, France*
[e] *Université de Toulouse, CNRS, Institut de Chimie de Toulouse ICT - UAR2599, 118 Route de Narbonne, 31062 Toulouse, France*

† Electronic supplementary information (ESI) available: Experimental and computational details and cif file for X-ray diffraction analysis. CCDC 2424974 and 2424975. For ESI and crystallographic data in CIF or other electronic format see DOI: https://doi.org/10.1039/d5cc02019k

‡ Both authors contributed equally to this work.

(Scheme 1A, eqn (2)). Although catalytic versions of *in situ* generated carbene and CO coupling have been developed for the synthesis of ketenes,[10] iron-based catalysts are presently unknown. Conversely, bridging iron nucleophilic alkylidenes follow different pathways.[11] They primarily react as (double) alkyl ligands, undergoing CO migratory insertion. The resulting acyl ligands are then transformed into a variety of compounds by migratory insertion of alkenes and alkynes, and oxidation. Upon solvolysis of the acyl with alcohols, esters are obtained (Scheme 1B, eqn (3)[12] and (4)[13]), and ketene-type intermediates have been proposed. This reactivity of bridging alkylidenes with CO was mostly described with dimetallic iron^{I} compounds, generating iron^{0} byproducts. In the absence of appropriate ligand(s) on the iron, the reverse reaction is observed, and ketene derivatives would be decarbonylated by iron^{0} complexes to generate dimetallic iron^{I} alkylidene (Scheme 1B, eqn (5)).[14] Further stabilization by conjugation of the ketene would hamper this process, as exemplified by the abundance of iron^{0} vinylketene complexes in the literature.[15] The reluctance of bridging iron alkylidenes to liberate ketenes contrasts with the ability of cobalt analogues to catalyze the coupling of CO and diazo compounds, *via* bridging alkylidene intermediates.[6,10,16]

Our group has been using P-stabilized geminal dianions to build terminal and bridging alkylidene complexes of a variety of transition metals.[17] Most recently, we explored the reactivity of sulfur and carbon ligated di-iron bis-alkylidene complexes,[18] with the aim of developing synthetic nitrogenase mimics.[19,20] This platform effectively provided S- and C-based coordination sites to the iron, while introducing charge at the carbon centre. Its structural flexibility allowed for the stabilization of redox-stable poly-iron species, where the $(S\sim C\sim S)^{2-}$ ligand adopted a bridging alkylidene configuration. In this work, we explore the ability of carbonyl to promote a terminal iron alkylidene reactivity in di-iron bis-alkylidene complexes, *i.e.*, fast and quantitative CO/alkylidene coupling resulting in the formation and release of a ketene, and the role of iron oxidation states in promoting ketene decoordination in non-coordinating media.

Complexes **1** and **2** were synthesized following the reported procedure.[20] Subjecting a CH_2Cl_2 solution of complex **1** to **6** bar CO resulted instantaneously in a colour change from green to dark red (Scheme 1C). ^{1}H and ^{31}P{^{1}H} NMR monitoring proved complete conversion in 6 h at this pressure (3 days at 1 atm) to two diamagnetic compounds in a 1 : 1 ratio, as illustrated by the appearance of two singlets in ^{31}P{^{1}H} NMR, at 72.1 and 38.0 ppm (37.4 ppm in THF). The signal at 72.1 ppm could be attributed to (1κS^{1},2κS^{5}-μ^{2})-bis-(diphenylthiophosphinoyl)-methanediide di-iron hexacarbonyl complex **3**, as determined by X-Ray diffraction on crystals grown from the reaction medium. Complex **3** shows C1–Fe bond lengths in the range of C-bridged Fe alkylidene dimers (Fig. 1). The Fe–Fe bond length (2.626(2) Å) is very close to those in $(CF_3)_2C$ alkylidene,[14] $Ph_2C{=}C$ allenic alkylidene,[21] carbene substituted alkylidene,[22] or conjugated alkylidenes.[23] In ^{13}C{^{1}H} NMR, the alkylidene signal is seen as the expected high field triplet at 39.1 ppm (J_{C-P} = 21.7 Hz), attesting to the high residual negative charge on C. Five infra-red vibrations of CO ligands were seen at 2040 cm^{-1}, 1992 cm^{-1}, 1965 cm^{-1}, 1954 cm^{-1} and 1937 cm^{-1}. Complexes **1** and **3** obviously display quite different electronic structures, notably due to the change in the oxidation states of the Fe centres. To describe these in a more detailed way, we have performed multiconfigurational electronic structure theory calculations (see ESI† for details). In complex **1**, we have confirmed the high-spin characters of the Fe^{II} centres, the antiferromagnetic coupling between these while locked in their ground orbital configurations, and the potential importance of near-orbital degeneracies on the magnetism of this compound. Complex **3** is a closed-shell system, best described as a σ-bonded di-iron complex, with an effective Fe–Fe bond order[24] of 0.77, which is indicative of a single bond. This depiction is in line with the Mössbauer spectra (see ESI†), which can be simulated with a unique set of parameters. The low isomer shift of 0.07 mm s^{-1} is consistent with an Fe^{I} coordinated to strong π-acceptor ligands (the three CO molecules),[25] while the magnetic Mössbauer spectra elicit simulation with an S = 0 Hamiltonian, consistent with the covalent coupling described earlier.

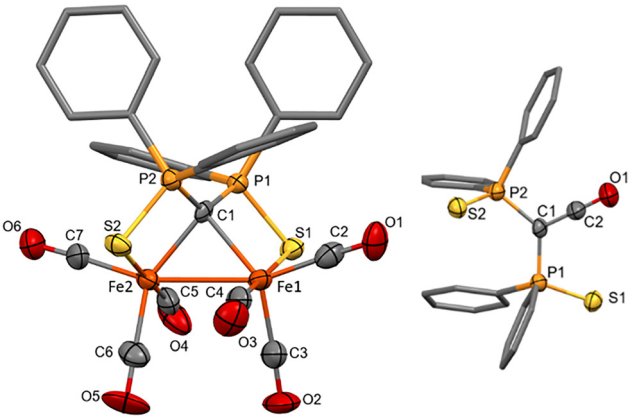

Fig. 1 X-Ray diffraction structure of μ^{2}-alkylidene iron(I) complex **3** (left) and ketene **4** (right). Thermal ellipsoids are represented at 50% probability level. H atoms are omitted for clarity. Selected bond lengths (Å) for **3**: Fe1–Fe2 2.626(2), Fe1–C1 2.046(8), Fe2–C1 2.032(9), Fe1–C2 1.782(12), Fe1–C3 1.794(11), Fe1–C4 1.740(11), Fe1–S1 2.408(3), Fe2–C5 1.736(12), Fe2–C6 1.794(11), Fe2–C7 1.788(11) Fe2–S2 2.415(3); for **4**: O1–C2 1.184(6), C2–C1 1.280(6), C1–P1 1.818(4), C1–P2 1.801(4).

Along with red crystals of complex **3**, colourless needles formed spontaneously in the crude mixture, corresponding to the 38.0 ppm signal as shown by ^{31}P{^{1}H} NMR of the redissolved crystals. Compound **4** is an unusual example of a room temperature stable ketene. According to X-Ray diffraction (Fig. 1), its C═C and C═O bond distances of 1.280(6) Å and 1.184(6) Å are close to those observed in typical examples of stable ketenes, such as Mes_2CCO and $(3,5\text{-}Br_2\text{-}2,4,6\text{-}Me_3Ph)_2CCO$ (1.29(1) Å and 1.25(3) Å for C═C bond lengths, and 1.18(1) Å and 1.17(3) Å for C═O bond lengths, respectively),[26] and those in the only rare examples of $Ph_2P(S)$-substituted ketenes **5-E**[27] (Scheme 2 eqn (7), $d_{C=C}$ being 1.304(2) Å, E = TMS, 1.314(5) Å, E = Ph_3C, and $d_{C=O}$ being 1.162(2) Å, R = TMS, and 1.166(5) Å, R = Ph_3C). The ^{13}C{^{1}H} NMR chemical shifts for C*C*O and P*C*P (181.9 ppm, resp. 38.1 ppm, t, $^{1}J_{PC}$ = 106 Hz) in **4** are very close to those of **5-CPh$_3$** (182.0 ppm, resp. 45.3 ppm). A sharp and intense absorption at 2112 cm^{-1} is seen in IR spectroscopy for the stretching of the CO bond.

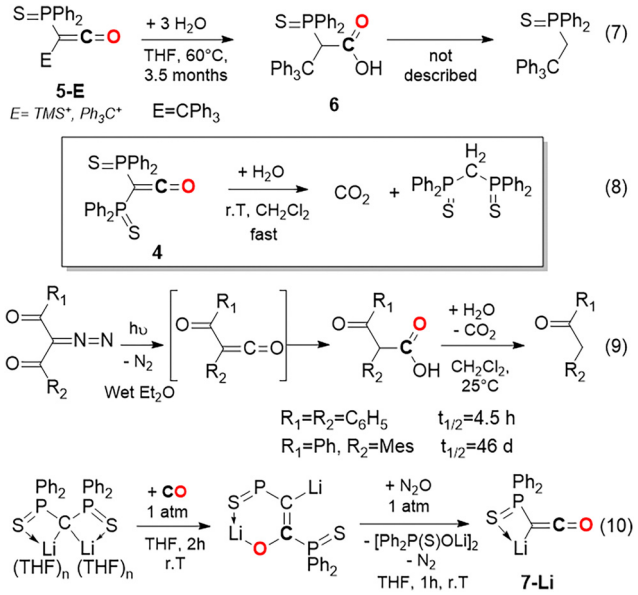

Scheme 2 Comparative reactivity of ketenes obtained from methanediide, yldiide, or 2-diazo-1,3-diketone, and the reactivity of dilithiated methanediide with CO.

We evaluated its reactivity as an electrophilic species. In stark contrast with what was described for **5-CPh$_3$**, which needed prolonged heating in presence of water (3.5 months at 60 °C) to be converted to the corresponding carboxylic acid **6** (Scheme 2, eqn (7)), ketene **4** proved to undergo instantaneous decarboxylation upon the addition of traces of water, to generate the neutral, doubly protonated bis (thiophosphinoyl)-methane ligand precursor (Scheme 2, eqn (8)). CO_2 evolution was confirmed by gas chromatography (see ESI†). If the effect of steric hindrance on the kinetics of hydration/decarboxylation of α-ketoketene has been documented (Scheme 2, eqn (9)),[28] the electronic effects of a second strongly electron withdrawing "Ph_2PS" moiety should be considered as well to explain the impressive difference in reactivity between **5-E** and **4**. The lability of the newly formed C=C bond is promising for a post-functionalisation of the carbon centre originating from CO. The easy formation of ketene **4** from the bis-μ^2-alkylidene complex **2** also contrasts with the known reactivity of the free, dilithiated $(S\sim C\sim S)^{2-}$ ligand toward CO, which was shown to undergo CO insertion into one CP bond[29] (Scheme 2, eqn (10)). In a similar way, related ylide species[27] lead to ketenyl anion **7-K** *via* breaking of one C–P bond. With the aim of identifying intermediates of the conversion of **1** to **3** and **4**, low temperature NMR experiments were carried out. At the early stage of the reaction between **2** and CO at −40 °C, two sets of two doublets were observed in a 1 : 1 : 1 : 1 ratio (75.6 ppm, 56.2 ppm, J_{PP} = 14 Hz, 65.8 ppm, 30.4 ppm, J_{PP} = 58 Hz) in $^{31}P\{^1H\}$ NMR. Such displacements are consistent with cyclometallated and carbonylated diphenyl-thiophosphinoyl-ylide ligands.[30–33] A 2D experiment as well as selective decoupling allowed the signals at 75.6 and 56.2 ppm in $^{31}P\{^1H\}$ NMR to be correlated with a carbon resonance at 34.3 ppm in $^{13}C\{^1H\}$ NMR, close to the displacement of the alkylidene carbon in **3**. The signals at 65.8 and 30.4 ppm in $^{31}P\{^1H\}$ NMR correlated with a doublet of doublets at 87.2 ppm and two

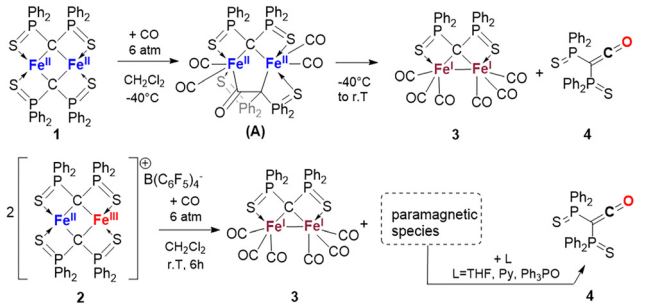

Scheme 3 Possible reaction paths for the formation of **3** and **4** from **1** and **2**.

multiplets at 206 and 224 ppm in $^{13}C\{^1H\}$ NMR. Similar ^{13}C NMR displacement at 226 ppm was already observed for a conjugated acyl coordinated to iron(II) carbonyl complexes.[34] This ^{13}C-NMR signature is consistent with the product of 1,1 migratory insertion of CO in one Fe–C bond. Three non-^{31}P-coupled, coordinated CO resonances were also seen. These observations are thus in accordance with structure **A** (Scheme 3). Evolution of complex **A** directly leads to the formation of complex **3** and the ketene compound **4** upon warming to room temperature.

To our surprise, when complex **2** was reacted with CO in CH_2Cl_2, compound **3** proved to be the only diamagnetic compound in solution. Its isolated yield was measured to represent *ca.* 50% of the starting iron, suggesting the concomitant formation of paramagnetic Fe complex(es). This was confirmed by Evan's method (see ESI†). As only one $(S\sim C\sim S)^{2-}$ ligand is bound to complex **3**, the other S∼C∼S moiety has to be bound to the paramagnetic Fe centre(s). Consistently, changing the solvent from non-coordinating CD_2Cl_2 to coordinating solvents such as THF-d_8 or CD_3CN led to the appearance of the ^{31}P NMR diamagnetic signal of **4** in a 2 : 1 ratio compared to **3**. Multiple solvent change cycles (THF-d_8 to CD_2Cl_2, then CD_2Cl_2 to THF-d_8) demonstrated the reversibility of this decoordination/coordination process of compound **4**. Classical L-type ligands such as pyridine and triphenylphosphine oxide were also able to displace **4**. The by-product(s) of this reaction were reluctant to crystallise and difficult to analyse by NMR due to their highly paramagnetic nature. The IR (ATR) spectrum revealed a sharp absorption at 2132 cm^{-1} corresponding to CCO bond stretching, demonstrating coordination of the ketene species **4** to the Fe centre. Coordinated CO absorption bands at 1981, 2036 and 2072 cm^{-1} were also seen. This last high value of ν_{CO} is reminiscent of cationic, thioether bonded Fe^{II} carbonyl complexes,[35] and other Fe^{II} coordinated by poor donor ligands.[36,37] Intense signals for the $B(C_6F_5)_4^-$ anion were also present. No active species was seen in X-band EPR spectroscopy, excluding the presence of Fe^{III} centres. These findings are consistent with the low-field Mössbauer spectrum of the by-products (see ESI†), which shows a very broad main doublet with a 0.95 mm s^{-1} isomer shift characteristic of adventitiously-bound Fe^{II} accompanied by a minor doublet (∼30% in Fe content) with a low isomer shift of 0.11 mm s^{-1}, which can be assigned to an Fe^{I}-carbonyl species different from **3**. These elements pointed to polymetallic, cationic iron oligomers featuring both several CO and ketene ligands.

To illustrate the relative reluctancy of ketene release in the case of $Fe^{I}Fe^{II}$ compounds, preliminary DFT calculations were performed. The $H_2C{=}C{=}O$ ketene was chosen to simplify the calculations. As the starting complexes are not known, we based our analysis on initial $Fe^{I}Fe^{II}$ and $Fe^{I}Fe^{I}$ complexes derived from **3** by substituting one CO ligand by the model ketene (see ESI†). From this study, we confirm that ketenes have a better affinity for $Fe^{I}Fe^{II}$ complexes than for $Fe^{I}Fe^{I}$ ones. Note that while the ketene binds on localized Fe^{II} sites in the initial $Fe^{I}Fe^{II}$ complex, the final $Fe^{I}Fe^{II}$ complex is valence delocalized; the ketene thus acts here as a "localization enforcer".

In conclusion, a bridging iron alkylidene complex featuring $(S\sim C\sim S)^{2-}$ ligands was able to release a stable ketene upon reaction with CO, under moderate pressure and at room temperature. This transformation can be performed from the neutral, bis-ferrous alkylidene complex **1**, generating the μ^2-alkylidene di-iron hexacarbonyl complex **3** as a by-product, or its mixed-valence analogue **2**. In the latter case, retention of the ketene moiety highlighted the impact of the oxidation state of iron on its release. The facile and complete cleavage of the newly formed C=C bond upon hydrolysis opens up new perspectives for the development of further reactivity, using the *gem*-dianion as a mediator for CO incorporation.

SM and RRM thank the ANR for financial support (ANR-21-CE07-0007, ENigM). CalMip is acknowledged by MFB for a generous grant of computing time. The ICT NMR service members are gratefully acknowledged for their technical support. RGS thanks Labex Arcane, CBH-EUR-GS (ANR-17-EURE-0003) for financial support.

Data availability

X-ray crystallographic data have been deposited in the Cambridge Crystallographic Data Centre (**https://www.ccdc.cam.ac.uk/**) with reference numbers: CCDC 2424974 (3) and 2424975 (4).† Experimental data and computational details have been included as part of the ESI.†

Conflicts of interest

There are no conflicts to declare.

Notes and references

1 W. A. Herrmann, *Angew. Chem., Int. Ed. Engl.*, 1982, **21**, 117–130.
2 X. Yin and J. R. Moss, *Coord. Chem. Rev.*, 1999, **181**, 27–59.
3 J. Pospech, I. Fleischer, R. Franke, S. Buchholz and M. Beller, *Angew. Chem., Int. Ed.*, 2013, **52**, 2852–2872.
4 S. Pandey, K. V. Raj, D. R. Shinde, K. Vanka, V. Kashyap, S. Kurungot, C. P. Vinod and S. H. Chikkali, *J. Am. Chem. Soc.*, 2018, **140**, 4430–4439.
5 T. W. Bodnar and A. R. Cutler, *J. Am. Chem. Soc.*, 1983, **105**, 5926–5928.
6 Z. Zhang, Y. Zhang and J. Wang, *ACS Catal.*, 2011, **1**, 1621–1630.
7 S. K. Russell, J. M. Hoyt, S. C. Bart, C. Milsmann, S. C. Stieber, S. P. Semproni, S. DeBeer and P. J. Chirik, *Chem. Sci.*, 2014, **5**, 1168–1174.
8 S. Takebayashi, M. A. Iron, M. Feller, O. Rivada-Wheelaghan, G. Leitus, Y. Diskin-Posner, L. J. W. Shimon, L. Avram, R. Carmieli, S. G. Wolf, I. Cohen-Ofri, R. A. Sanguramath, R. Shenhar, M. Eisen and D. Milstein, *Nat. Catal.*, 2022, **5**, 494–502.
9 Q. Wang, R. A. Manzano, H. Tinnermann, S. Sung, B. Leforestier, T. Krämer and R. D. Young, *Angew. Chem., Int. Ed.*, 2021, **60**, 18168–18177.
10 T. R. Roose, D. S. Verdoorn, P. Mampuys, E. Ruijter, B. U. W. Maes and R. V. A. Orru, *Chem. Soc. Rev.*, 2022, **51**, 5842–5877.
11 R. Mazzoni, M. Salmi and V. Zanotti, *Chem. – Eur. J.*, 2012, **18**, 10174–10194.
12 M. Röper, H. Strutz and W. Keim, *J. Organomet. Chem.*, 1981, **219**, C5–C8.
13 B. Denise, D. Navarre, H. Rudler and J. C. Daran, *J. Organomet. Chem.*, 1989, **375**, 273–289.
14 M. Wiederhold and U. Behrens, *J. Organomet. Chem.*, 1994, **476**, 101–109.
15 S. E. Gibson and M. A. Peplow, In *Advances in Organometallic Chemistry*, ed R. West, A. F. Hill, Academic Press, 1999, vol. 44, pp. 275–355.
16 T. Kegl and F. Ungvary, *Lett. Org. Chem.*, 2010, **7**, 634–644.
17 M. Fustier-Boutignon, N. Nebra and N. Mézailles, *Chem. Rev.*, 2019, **119**, 8555–8700.
18 M. Fustier-Boutignon, H. Heuclin, X. F. Le Goff and N. Mézailles, *Chem. Commun.*, 2012, **48**, 3306–3308.
19 S. Yogendra, D. W. N. Wilson, A. W. Hahn, T. Weyhermüller, C. Van Stappen, P. Holland and S. DeBeer, *Inorg. Chem.*, 2023, **62**, 2663–2671.
20 R. Ravel-Massol, S. Munshi, A. Pujol, R. Garcia-Serres, N. Saffon-Merceron, N. Mézailles and M. Fustier-Boutignon, *Chem. – Eur. J.*, 2023, **29**, e202302130.
21 O. S. Mills and A. D. Redhouse, *J. Chem. Soc. A*, 1968, 1282–1292.
22 J. C. Daran, B. Heim, M. Gouygou and Y. Jeannin, *J. Organomet. Chem.*, 1994, **479**, 109–116.
23 S. Bernès, R. A. Toscano, A. C. Cano, O. G. Mellado, C. Alvarez-Toledano, H. Rudler and J.-C. Daran, *J. Organomet. Chem.*, 1995, **498**, 15–24.
24 B. O. Roos, A. C. Borin and L. Gagliardi, *Angew. Chem., Int. Ed.*, 2007, **46**, 1469–1472.
25 S. A. Stoian, C.-H. Hsieh, M. L. Singleton, A. F. Casuras, M. Y. Darensbourg, K. McNeely, K. Sweely and C. V. Popescu, *J. Biol. Inorg. Chem.*, 2013, **18**, 609–622.
26 S. E. Biali, M. Gozin and Z. Rappoport, *J. Phys. Org. Chem.*, 1989, **2**, 271–280.
27 M. Jörges, F. Krischer and V. H. Gessner, *Science*, 2022, **378**, 1331–1336.
28 H. Meier, H. Wengenroth, W. Lauer and V. Krause, *Tetrahedron Lett.*, 1989, **30**, 5253–5256.
29 M. Xu, T. Wang, Z.-W. Qu, S. Grimme and D. W. Stephan, *Angew. Chem., Int. Ed.*, 2021, **60**, 25281–25285.
30 E. Lindner, A. Rau and S. Hoehne, *Angew. Chem.*, 1979, **91**, 568–569.
31 J. Weismann and V. H. Gessner, *Eur. J. Inorg. Chem.*, 2015, 4192–4198.
32 P. Oulié, N. Nebra, S. Ladeira, B. Martin-Vaca and D. Bourissou, *Organometallics*, 2011, **30**, 6416–6422.
33 J.-Y. Guo, Y. Li, R. Ganguly and C.-W. So, *Organometallics*, 2012, **31**, 3888–3893.
34 C. P. Casey, L. K. Woo, P. J. Fagan, R. E. Palermo and B. R. Adams, *Organometallics*, 1987, **6**, 447–454.
35 D. Sellmann, G. Mahr, F. Knoch and M. Moll, *Inorg. Chim. Acta*, 1994, **224**, 45–59.
36 T. S. Piper, F. A. Cotton and G. Wilkinson, *J. Inorg. Nucl. Chem.*, 1955, **1**, 165–174.
37 F. A. Cotton and B. F. G. Johnson, *Inorg. Chem.*, 1967, **6**, 2113–2115.

